Desalination and Water Treatment
www.deswater.com

doi:10.5004/dwt.2016.0218

66 (2017) 330–337
March

Preparation and photocatalytic activity of porous ZnO and Cr^{3+} doped ZnO microparticles

Yuan Cao*, Xianling Li, Ling Hu, Peiyuan Wang, Yanqin Xu

College of Chemistry and Chemical Engineering, Chongqing University, Chongqing 400044, China, Tel. +86 15923344273, Fax +86 23 65111748, email: caoyuan108@vip.sina.com, caoyuan@cqu.edu.cn (Y. Cao), Tel. +86 18875208031, email: lxllastone@sina.com (X. Li), 928336402@qq.com (L. Hu), wangpeiyuan2012@163.com (P. Wang), xuyanqin666@163.com (Y.Xu)

Received 25 February 2016; Accepted 16 June 2016

ABSTRACT

In this study, the porous flowerlike ZnO and Cr^{3+} doped ZnO (Cr^{3+} = 1 mol%, 2 mol% and 3 mol%) microparticles were successfully synthesized via a simple microwave irradiation process, their structural and photocatalytic properties were systematically investigated. The morphology, physicochemical properties, element state and crystal phase of prepared catalysts were characterized by SEM, XRD, XPS, N_2 adsorption-desorption and AAS, respectively. Besides, the photocatalytic decomposition of Methylene Orange (MO) under solar irradiation also was employed to measure the photocatalytic properties of the pure ZnO and Cr^{3+} doped ZnO catalysts. The effects of degradation time, Cr^{3+} doped contents, amount of catalyst, initial dye concentration and pH on photocatalytic activities were analyzed. The results proved that the approach assisted by microwave irradiation was efficient for preparation of microparticles with good morphology, the photocatalytic properties of the obtained ZnO have been greatly improved through doping with Cr^{3+}. And the photocatalytic degradation ratio can reach to 99%, when the doping content of Cr^{3+} is 2 mol%, pH = 5, after reacting for 150 min. At last, the mechanism of photocatalytic degradation of MO was studied by trapping experiments.

Keywords: ZnO; Porous; Cr^{3+} doped; Microwave irradiation; Photocatalytic activities

1. Introduction

Zinc oxide, which is a significant II–IV semiconductor [1] with a wide band gap (3.37 eV) and large exciton binding energy (60 meV), has received great attentions because of its promising applications in optoelectronics, field emitters, sensors, transistors and photocatalysts [2–5]. Due to these applications, a variety of nano-structural ZnO had been fabricated, such as nanorods, nanowires, nanotubes and nanospheres [6–10].

TiO_2 has been widely used for photocatalyst for many years. Compared with TiO_2, ZnO has more advantages, such as lower cost, higher photocatalytic efficiencies and larger quantum efficiency [11,12]. Therefore, ZnO can be a suitable alternative photocatalyst to TiO_2 as they have similar band gap energy. The band gap energy of ZnO is 3.37 eV, makes ZnO only absorb UV light that is less than 10% in the solar irradiation [13–15]. In order to absorb more visible light to improve the photocatalytic efficiency, the band gap of ZnO has to be narrowed or split into several sub-gaps, which can be achieved by implanting or doping transition metal ions. To date, there are many studies about the properties and applications of ZnO doped with different elements, such as Co^{2+}, Mn^{2+} and Cr^{3+} [16–18].

Many methods have been developed for the fabrication of ZnO nanoparticles including the thermal evaporation, chemical vapor deposition, sol-gel method, hydrothermal method and electrochemical deposition [19–25] in the past decades. However, several studies have reported the synthesis of porous ZnO using microwave irradiation. The process assisted by microwave irradiation exhibits varieties of merits including uniform and volumetric heating, fast

*Corresponding author.

kinetics and energy saving [26,27]. Therefore, synthesis of nano ZnO, as well as other metal oxide, assisted by microwave can be desirably employed in the future.

In this paper, we report an efficient and convenient approach to produce well-aligned porous flowerlike ZnO and Cr^{3+} doped ZnO microparticles under microwave irradiation. We try to dope Cr^{3+} in ZnO to narrow the band gap or split into sub-gaps in ZnO to improve its photocatalytic activities. Moreover, the photocatalytic ability and photodecomposition mechanism of Cr^{3+} doped ZnO were carefully studied by decomposition of MO under solar light.

2. Experiment

2.1. Synthesis of ZnO and Cr^{3+} doped ZnO

The preparation method assisted by microwave irradiation was successfully applied to synthesize ZnO and Cr^{3+} doped ZnO (Cr^{3+} = 1 mol%, 2 mol% and 3 mol%) powders. In the typical procedure, zinc acetate dehydrate (0.01 mol) and different molar ratios of chromium acetate hexahydrate (n_{Cr}:n_{Zn} = 0 mol%, 1 mol%, 2 mol% and 3 mol%) were dissolved in 30mL distilled water with continuously stirring to dissolve entirely. Then sodium hydrate solution (2 mol/L) as the precipitation agent was added slowly into the above clear solution under stirring until the pH of the solution reach to 9, precursor had been prepared. Afterwards, the as-obtained precursor was placed into a domestic microwave oven (800 W, 2450 MHz, Galanz). The power of the microwave oven was 320 W and the irradiation time was 30 min. After boiling, evaporating and concentrating during the irradiation process, the ZnO and Cr^{3+} doped ZnO microparticles were obtained (0% Cr-ZnO, 1% Cr-ZnO, 2% Cr-ZnO, 3% Cr-ZnO represent the doping contents of Cr^{3+} was 0 mol%, 1 mol%, 2 mol%, 3 mol%, respectively).

2.2. Characterization

The structure and crystal phase were characterized by X-ray diffraction (XRD, Shimadzu XRD-6000 with Cu Kα radiation, 40 kV, 30mA).The morphologies and the size of the samples were measured via scanning electron microscopy (SEM, JEOL JSM-6490LV). The Brunauer-Emmett-Teller (BET) specific surface area (S_{BET}) and BJH pore distribution of the powders were measured using a nitrogen adsorption/desorption apparatus (ASAP 2020).The elements state was measured by X-ray photoelectron spectroscopy (XSAM800). The actual concentration of Cr^{3+} was measured by atomic absorption spectrophotometer (WFX-110). The degradation efficiency was detected by UV-vis spectrophotometer (UV2600).

2.3. Photocatalytic activity test

The photocatalytic activity of ZnO and Cr^{3+} doped ZnO catalysts were measured by decomposition of MO, whose degradation can be easily monitored by optical absorption spectroscopy. The photocatalytic activity tests were all conducted in a 25 ml colorimetric tube, in which a certain amount of catalyst and certain concentration of 25 ml MO (4–16 mg/L) were added. The tube was put on a magnetic stirrer, before exposure to light source, and the suspensions were stirred for 30 min in the dark to attain the adsorption-desorption aquilibruim. Then suspensions were stirred for 150 min in solar illumination. The reaction was carried out at room temperature and pH = 3–8, while pH was changed by adding either NaOH or HCl solution. The comparing experiment, the MO solution is illuminated under the solar irradiation without photocatalyst. The photocatalytic degradation was measured by the absorbance of the solution samples with a UV-vis spectrophotometer at λ_{max} = 463 nm. The photocatalytic decomposition of MO was calculated by the equation: degradation ratio (%) =$[C_o–C]/C_o \times 100\%$. C_o and C are the initial and final concentration of MO, respectively.

2.4. Evaluation of photocatalytic activity and trapping experiments for reactive species

The durability and stability test was also conducted by following similar approach as discussed earlier (MO 8 mg/L). Three consecutive cycles, in which the duration of each cycle was 150 min, were performed on as-prepared 2% Cr-ZnO (0.2 g) photocatalysts. After the each end of cycle, the product was filtrated and washed with deionized water. It was then added to the new MO solution after drying. The photocatalytic result was performed at least two experimental runs, using the average value to determine the durability and stability of 2% Cr-ZnO.

The influence of various reactive species such as holes (h^+), electrons (e^-), hydroxyl (·OH), and superoxide ($\cdot O_2^-$) radicals on the MO degradation was examined to understand the photocatalytic mechanism in the 2% Cr-ZnO system. Various scavenging reagents such as triethanolamine (TEOA, h^+ scavenger), silver nitrate ($AgNO_3$, e^- scavenger), isopropanol (IPA, ·OH scavenger), and benzoquinone (BQ, $\cdot O_2^-$ scavenger) were used in this study. The concentrations of each scavenging reagent in the reaction system were all 24 mmol (MO 8 mg/L). The analysis procedure was exactly identical to the photodegradation process.

3. Results and discussions

3.1. XRD analysis

The typical XRD patterns of ZnO and Cr^{3+} doped ZnO microparticles are shown in Fig. 1. The labeled peaks are consistent with those of hexagonal wurtzite structure (JCPDS data: 36–451), indicates that the samples are highly crystalline and the doped Cr^{3+} has little effects on the polycrystalline structure. In addition, it is observed no characteristic peaks belonging to chromium oxide in all patterns, which demonstrates that Cr^{3+} was incorporated into the lattice well [28].

3.2. N_2 adsorption-desorption analysis

The N_2 adsorption-desorption isotherm and pore size distribution curves of ZnO and Cr^{3+} doped ZnO powders has been showed in Fig. 2a,b, the physicochemical properties of all the as prepared photocatalysts are depicted in Table 1. The Fig. 1 clearly reveals that all these samples

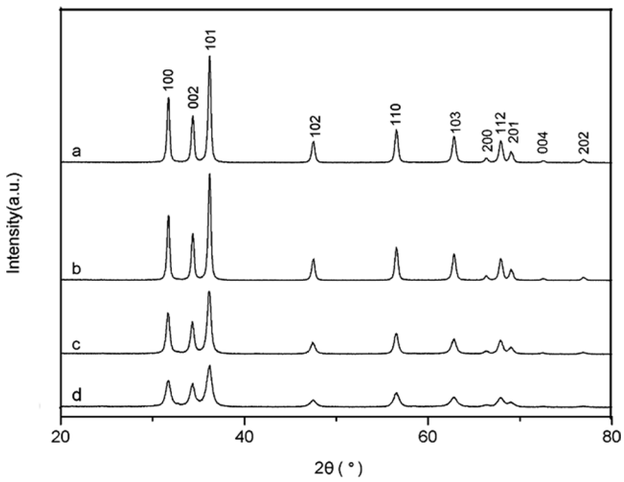

Fig. 1. XRD patterns of ZnO and Cr^{3+} doped ZnO microparticles. (a) 0% Cr-ZnO (b) 1% Cr-ZnO (c) 2% Cr-ZnO (d) 3%Cr-ZnO.

Table 1
Specific surface, pore volume and pore size

Samples	Surface area (BET m^2/g)	Pore volume (BJH adsorption cm^3/g)	Pore size (BET adsorption nm)
0% Cr-ZnO	18.4652	0.035095	7.60224
1% Cr-ZnO	22.3544	0.040946	7.32665
2% Cr-ZnO	36.1935	0.069233	7.65146
3% Cr-ZnO	65.2631	0.139975	8.57913

exhibit type Ⅰ and type Ⅱ isotherm, and its hysteresis loop indicates type H3 (according to IUPAC nomenclature) suggesting that there are microporous, mesoporous and macroporous in the materials. The pore size distribution curves (Fig. 2b) show that with the increase of Cr^{3+}, the pore size is transferred from the main microporous to the mesoporous. Table 1 indicates that the surface area, pore volume and pore size of photocatalyst all increase with the increasing of Cr^{3+}.

3.3. SEM analysis

Fig. 3 represents the SEM images of ZnO and Cr^{3+} doped ZnO. It can be observed that the structure of pure ZnO product is flowerlike in Fig. 3a. Fig. 3b–d show the SEM images of 1% Cr-ZnO, 2% Cr-ZnO and 3% Cr-ZnO respectively. As shown in these three images, the flakes of flower which are accumulated by ZnO nanoparticles, are destroyed after doping Cr^{3+} and the disorder network structure is formed. It is precisely because of this disordered network structure, the bulkiness and porosity of catalyst are improved. A closer inspection of the spherical structures (Fig. 3e,f) shows that the flakes and network structure are accumulated by the ZnO nanoparticles with size of 30 to 100 nm, with the porous structure formed in the process, which explain the fact that microwave promotes the concentration of the pore distribution between the particles is attributed to the generation of particle with uniform size. The formed of disordered network structure leads to increase the gap between particles after Cr^{3+} doped, and subsequently improves the pore size of catalyst. The results of N_2 adsorption-desorption analysis are also consistent with SEM.

3.4. XPS analysis

X-ray photoelectron spectroscopy (XPS) was used to ascertain the presence of Cr and its oxidatior state in ZnO. The XPS survey spectrum in Fig. 4a indicates that the presence of Zn, O, C and Cr. The introduction of C is possible due to the decomposition of organic compounds. Fig. 4b shows high-resolution of the Cr 2p region. The core level binding energy observed for the Cr $2p_{3/2}$ primary peak at 577.6 eV indicates that Cr in its trivalent state [29]. The distinct two states of Cr ($2p_{3/2}$) and Cr ($2p_{1/2}$) observed at 577.6 eV and 586.7 eV can further proved it is Cr^{3+} and substitutes Zn positions in the lattice.

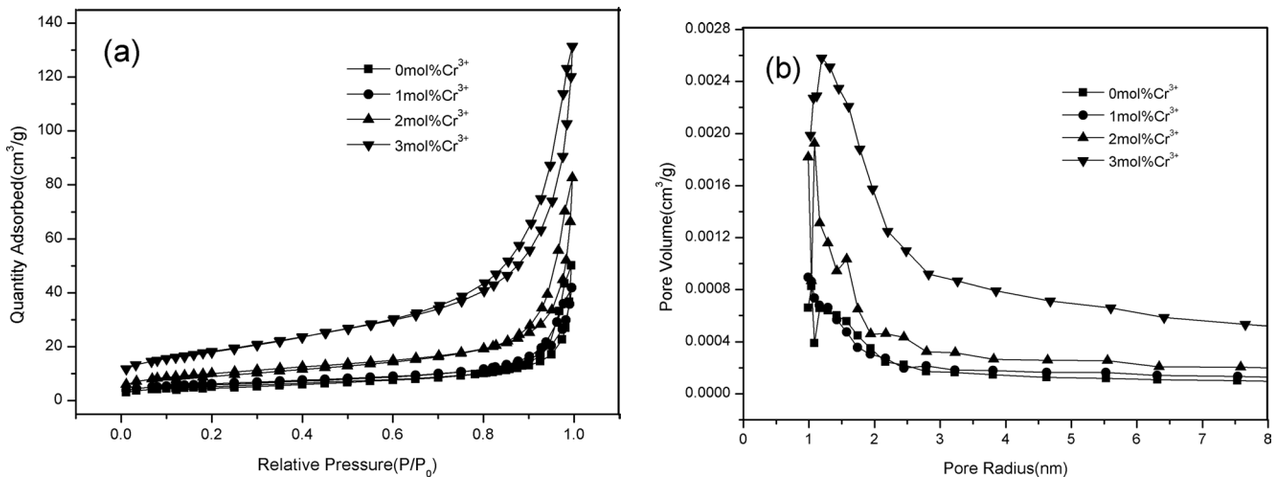

Fig. 2. N_2 adsorption-desorption study of ZnO and Cr^{3+} doped ZnO, (a) isotherm curves and (b) pore size distribution curves of ZnO with different Cr^{3+} doping contents.

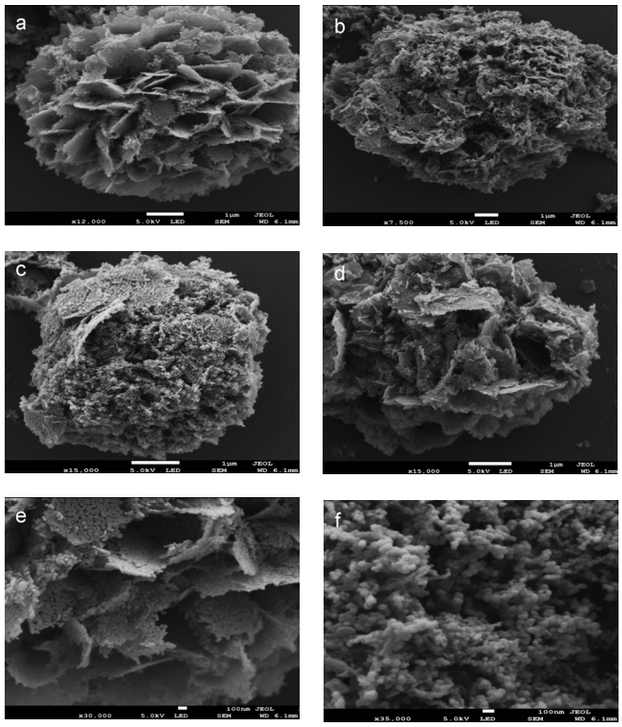

Fig. 3. SEM images of ZnO with different Cr^{3+} doping content: (a) 0% Cr-ZnO (b) 1% Cr-ZnO (c) 2% Cr-ZnO (d) 3% Cr-ZnO, and (e), (f) the local amplification of (a), (b).

3.5. AAS analysis

The actual content of Cr^{3+} doped in ZnO was shown in Table 2. It is seen that the actual content of Cr^{3+} was growing with the increased doping amount. There were not impurities for Cr^{3+} indicated in XRD figure, which stated that the Cr^{3+} was doped in ZnO well.

Table 2
Doped content of Cr^{3+} in ZnO

Catalyst	1% Cr-ZnO	2% Cr-ZnO	3% Cr-ZnO
Theoretical content (mol %)	1.00	2.00	3.00
Actual content (mol %)	0.93	1.89	2.88

3.6. Photocatalytic degradation of MO

3.6.1. Effect of doping concentrations on photocatalytic degradation efficiency

The effect of doping contents on the photocatalytic degradation efficiency is investigated with doping concentrations ranging from 0 mol% to 3 mol% and 4 mg/L MO concentration for 150 min. In the dark reaction process, the amount of MO reduction is very small, almost negligible. The curve of MO degradation ratio for photocatalysts of 0% Cr-ZnO, 1% Cr-ZnO, 2% Cr-ZnO and 3% Cr-ZnO microparticles (0.2 g) is shown in Fig. 5a, according to the curve, we can see that photocatalyst 2% Cr-ZnO exhibits higher photocatalytic efficiency than 1% Cr-ZnO and 3% Cr-ZnO. Fig. 5b shows the degradation efficiency of photocatalysts 0% Cr-ZnO and 1% Cr-ZnO in different time periods. It is seen obviously that the Cr^{3+} (1 mol%) doped ZnO photocatalyst presents much higher photocatalytic activity than the pure ZnO particles under solar irradiation, which may be attributed to the point defects of oxygen and zinc vacancies increased by heat treatment process via microwave and Cr^{3+} doping [30]. The photocatalytic activity enhancement by doping Cr^{3+} in ZnO can be explained to that the Cr-ZnO would produce electron-holes pairs under the solar light illumination. Cr^{3+} can act as photo-generates holes trappers to improve the transmission efficiency of photo induced carriers, which hinder the e^-–h^+ recombination in lattice and enhance the photocatalytic activity [31]. But, with the increase content of Cr^{3+} (exceed 2 mol%), the dispersion of Cr in ZnO matrix was reduced, and the formation of Cr_2O_3

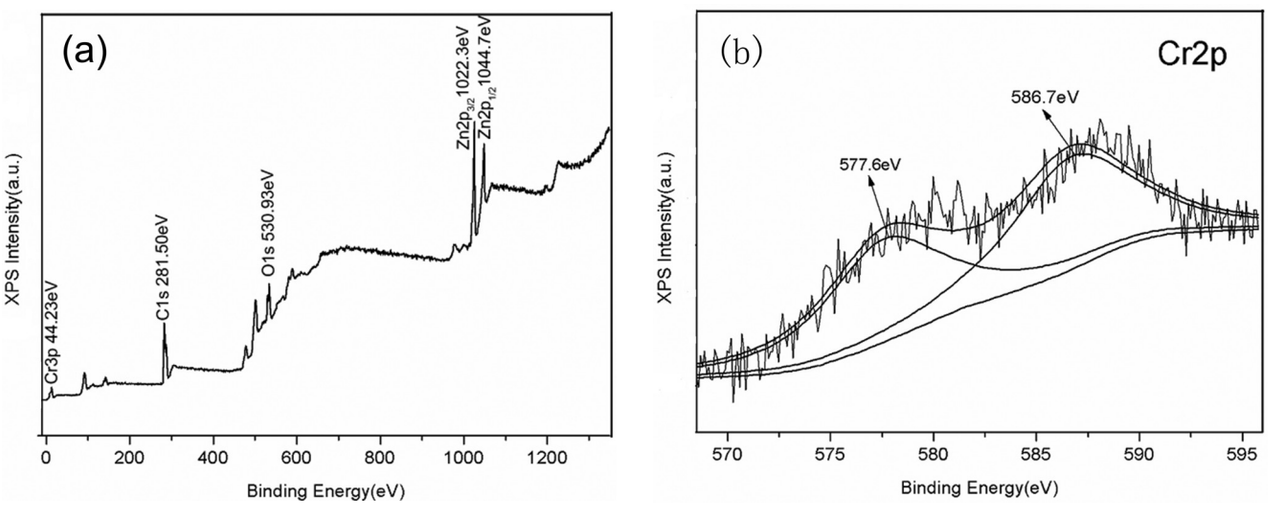

Fig. 4. XPS spectra of 2% Cr-ZnO: (a) XPS survey spectrum and (b) Cr 2p spectrum.

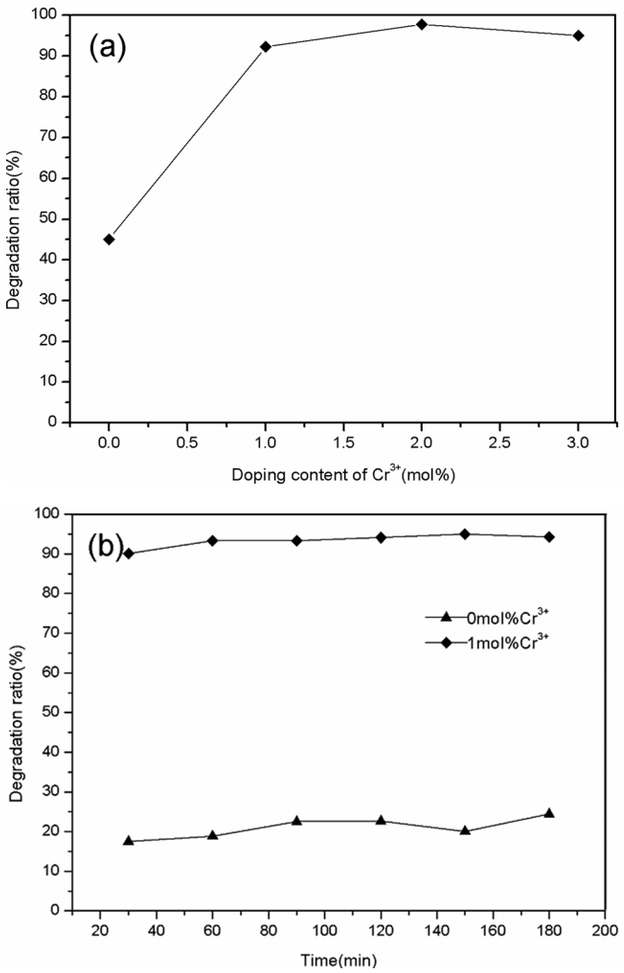

Fig. 5. Effect of (a) doping content of Cr^{3+} and (b) degradation time on the photocatalytic efficiency.

clusters was equivalent to aggregation center of e^- and h^+, which accelerated the recombination of e^- , h^+ and reduced the catalytic activity.

3.6.2. Effect of amount of catalyst on the photocatalytic efficiency

The amount of photocatalyst (2% Cr-ZnO) affects the overall degradation efficiency, when the MO concentration is 4 mg/L, in the photocatalytic system. As shown in Fig. 6, the photocatalytic efficiency rises with an increase of amount of catalyst until 2% Cr-ZnO increases above a saturation level. When the amount of catalyst exceeds 0.20 g, the degradation ratio of MO reduced, it is resulted from the decreasing coefficient of light photo absorption in this photocatalytic reactor (25 ml colorimetric tube) with certain diameter. And the excess 2% Cr-ZnO can form a light screen that reduces the surface area of ZnO being exposed to solar light illumination and reduces the photocatalytic efficiency. Therefore, in order to avoid excess catalyst and to ensure efficient photons absorption, the amount of catalyst can be appropriate to the photoreactor.

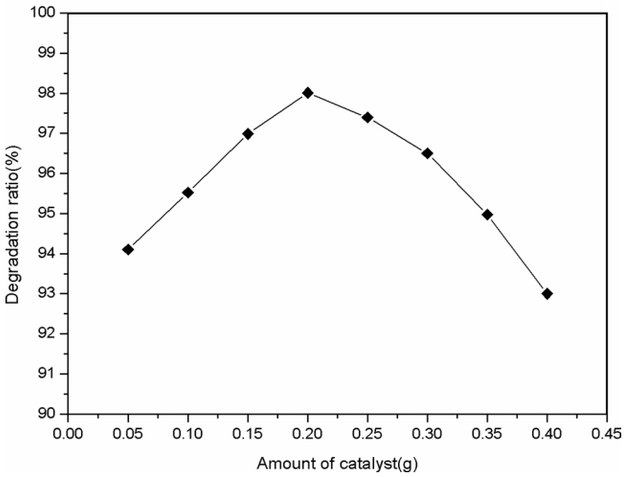

Fig. 6. Effect of amount of catalyst on the photocatalytic efficiency.

3.6.3. Effect of pH on photocatalytic efficiency

pH is one of the most important factors that affect the charge on the surface of photocatalyst particles and photocatalytic activities, which can be explained by zero-point charge depending on the catalyst used. As illustrated in Fig. 7, the degradation efficiency of MO (4 mg/L) in acid solution is higher than that in alkaline solution, with 2% Cr-ZnO 0.2 g. The maximum MO photocatalytic degradation 98.8% is achieved at pH of solution to be 5. The Zeta potential analysis shows (in Supplement Information) that the charged properties of 2% Cr-ZnO and MO are opposite, 2% Cr-ZnO has higher adsorption capacity, when pH = 3.62–7.00.

3.6.4. Effect of the concentration of MO on the photocatalytic efficiency

The effect of initial concentrations of MO on the photocatalytic degradation using 2% Cr-ZnO powder is investigated in the range of 4–16 mg/L. We studied their effects on photocatalytic degradation at 0.20 g and pH = 5 for 150 min. It also can be seen from Fig. 8 that the excessive con-

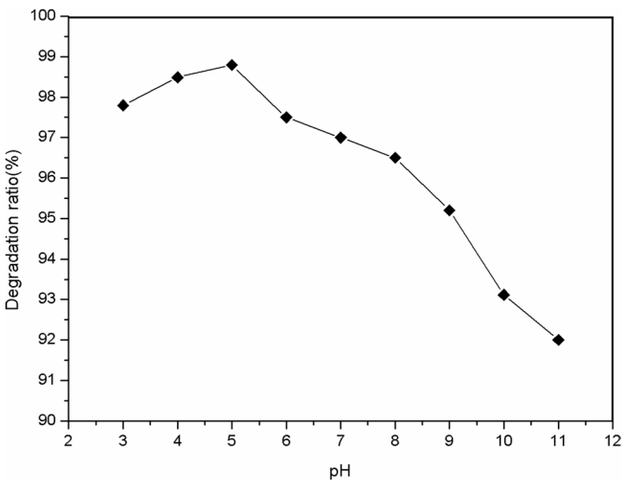

Fig. 7. Influence of pH on the photocatalytic efficiency.

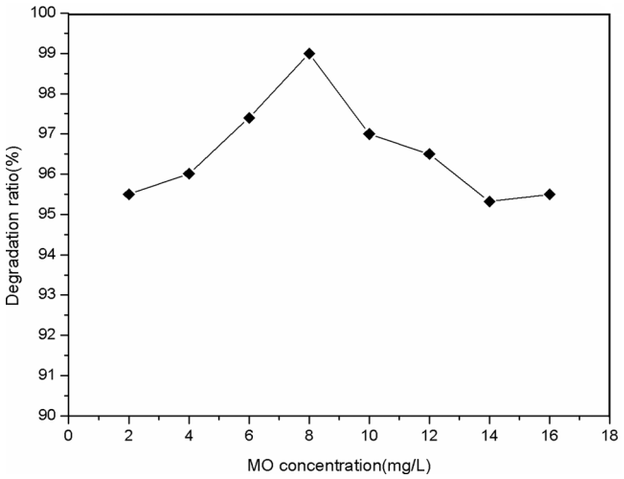

Fig. 8. Effect of initial concentrations of MO on the photocatalytic efficiency.

centration of MO will saturate the ZnO surface and reduce the photonic efficiency resulting photocatalyst deactivation. So, under similar reaction conditions, the best concentration of MO is 8 mg/L.

3.7. Stability and photocatalytic degradation mechanism analysis

The stability of a photocatalyst is also very important for point of view of its practical application. Hence, the stability of the 2% Cr-ZnO composite was further investigated by recycling the photocatalyst for degradation of MO. As shown in Fig. 9a, after three cycles (results are 90.2%, 89.7%, and 86.2% respectively), there is only a slight loss of activity. Therefore, the 2% Cr-ZnO composite can be used as high-performance and stable visible-light photocatalysts.

Detection of reactive species. The radicals, e^- and holes trapping experiments are designed to elucidate the photocatalytic oxidation process. Fig. 9b displays the effects of different scavengers on the degradation rate of MO degradation over the 2% Cr-ZnO composite. As depicted in Fig. 9b, the photoactivity was markedly suppressed as a result of the quenching effect. When BQ and $AgNO_3$ scavenger were added, the photocatalytic activity of 2% Cr-ZnO was reduced to 15.6% and 26.7% respectively, compared with no scavenger. The addition of IPA and TEOA scavengers also decreased photocatalytic activity smaller than the addition of BQ and $AgNO_3$. Therefore, it is evident that e^-, ·OH, holes and $\cdot O_2^-$ radicals all play important roles on the photodegradation of MO [32]. The photocatalytic degradation process is as follow:

$$Cr-ZnO \xrightarrow{hv} e^- + h^+ \quad (1)$$

$$e^- + O_2 \rightarrow \cdot O_2^- \quad (2)$$

$$\cdot O_2^- + 2H^+ + 2e^- \rightarrow \cdot OH + OH^- \quad (3)$$

$$h^+ + H_2O \rightarrow H^+ + \cdot OH \quad (4)$$

$$h^+ + OH^- \rightarrow \cdot OH \quad (5)$$

$$MO + h^+(\cdot O_2^-, \cdot OH \rightarrow \text{mineralized products} \quad (6)$$

4. Conclusion

We have developed an efficient method for preparation of ZnO powders with different Cr^{3+} doping contents through microwave irradiation. Characterization results show that the prepared photocatalysts are porosity, and the pore size increases with Cr^{3+}. The doping of Cr^{3+} has broken the flakes of flowerlike ZnO, but almost no influence on the crystalline phase of ZnO, which have the hexagonal wurtzite structure. The degradation results indicate that the doping Cr^{3+} can greatly improve the photocatalytic activities of ZnO under solar irradiation and the maximum photocata-

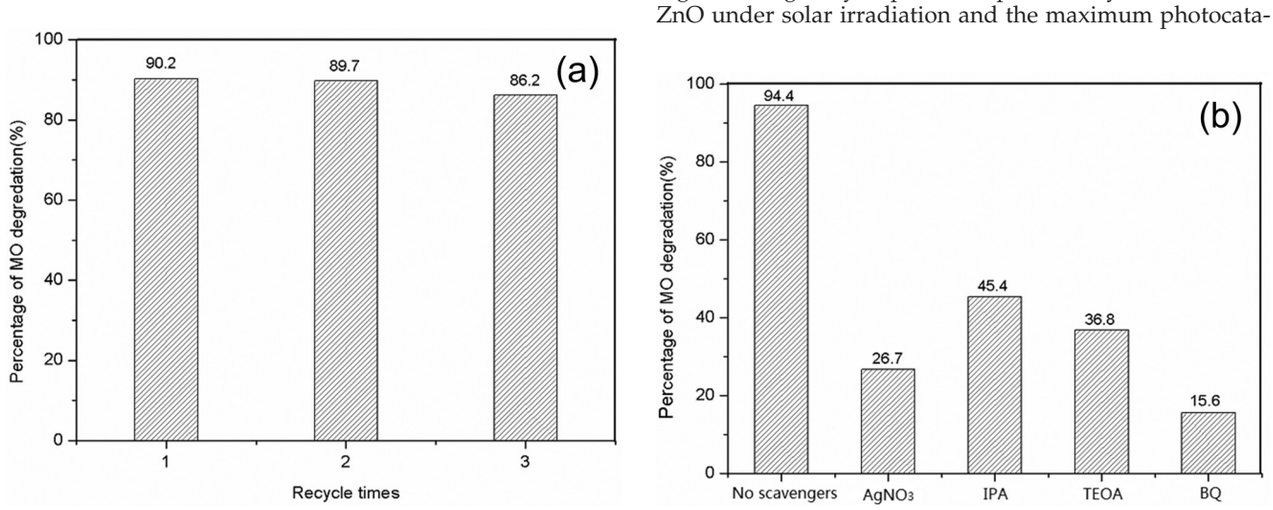

Fig. 9. (a) Recycling efficiency of 2% Cr-ZnO in the photocatalytic degradation of MO. (b) Effect of different scavengers on the MO photodegradation in the presence of 2% Cr-ZnO under solar light for 150 min.

lytic degradation (99%) of MO is achieved at pH = 5 with MO concentration 8 mg/L, solar irradiation for 150 min, when the doping concentration of Cr^{3+} is 2 mol%. It is suggested that Cr^{3+} in ZnO may be a promising breakthrough in the application of ZnO as photocatalysts. Moreover, we have proved that the oxidation state of chromium in 2% Cr-ZnO is Cr^{3+}, with low content and have no pollution to the environment.

Acknowledgments

We gratefully acknowledge funding from the Fundamental Research Funds for the Central Universities (CDJXS10221136)

References

[1] A. Janotti, C.G.V.D. Walle, Fundamentals of zinc oxide as a semiconductor, Rep. Prog. Phys., 72 (2009) 126–501.
[2] S. Chakrabarti, B.K. Dutta, Photocatalytic degradation of model textile dyes in wastewater using ZnO as semiconductor catalyst, J. Hazard. Mater., 112 (2004) 269–278.
[3] J. Goldberger, D.J. Sirbuly, M. Law, P. Yang, ZnO nanowire transistors, J. Phys. Chem. B, 109 (2005) 9–14.
[4] Y.P. Li, Y. Bando, D. Golberg, ZnO nanoneedles with tip surface perturbations: excellent field emitters, Appl. Phys. Lett., 84 (2004) 3603–3605.
[5] J. Xu, Q. Pan, Y. Shun, Z. Tian, Grain size control and gas sensing properties of ZnO gas sensor, Sensor Actuat. B-Chem., 66 (2000) 277–279.
[6] Y. Dai, Y. Zhang, Q.K. Li, C.W. Nan, Synthesis and optical properties of tetrapod-like zinc oxide nanorods, Chem. Phys. Lett., 358 (2002) 83–86.
[7] L. Vayssieres, K. Keis, A. Hagfeldt, S.E. Lindquist, Three-dimensional array of highly oriented crystalline ZnO microtubes, Chem. Mater., 13 (2001) 4395–4398.
[8] Q.C. Li, V. Kumar, Y. Li, H.T. Zhang, T.J. Marks, R.P.H. Chang, Fabrication of ZnO nanorods and nanotubes in aqueous solutions, Chem. Mater., 17 (2005) 1001–1006.
[9] J. Yu, X. Yu, Hydrothermal synthesis and photocatalytic activity of zinc oxide hollow spheres, Environ. Sci. Technol., 42 (2008) 4902–4907.
[10] Y.Z. Zhang, Y.P. Liu, L.H. Wu, H. Li, L.Z. Han, B.C. Wang, E.Q. Xie, Effect of annealing atmosphere on the photoluminescence of ZnO nanospheres, Appl. Surf. Sci., 255 (2009) 4801–4805.
[11] N. Daneshvar, D.Salari, A.R. Khataee, Photocatalytic degradation of azo dye acid red 14 in water on ZnO as an alternative catalyst to TiO_2, J. Photochem. Photobiol. A, 162 (2004) 317–322.
[12] L.K. Adams, D.Y. Lyon, P.J.J. Alvarez, Comparative eco-toxicity of nanoscale TiO_2, SiO_2, and ZnO water suspensions, Water. Res., 40 (2006) 3527–3532.
[13] S. Chakrabarti, B. Chaudhuri, S. Bhattacharjee, P. Das, B.K. Dutta, Degradation mechanism and kinetic model for photocatalytic oxidation of PVC–ZnO composite film in presence of a sensitizing dye and UV radiation, J. Hazard. Mater., 154 (2008) 230–236.
[14] T. Bak, J. Nowotny, M. Rekas, C.C. Sorrell, Photo-electrochemical hydrogen generation from water using solar energy. Materials-related aspects, Int. J. Hydrogen Energ., 27 (2002) 991–1022.
[15] H.F. Lin, S.C. Liao, S.W. Hung, The dc thermal plasma synthesis of ZnO nanoparticles for visible-light photocatalyst, J. Photochem. Photobiol. A, 174 (2005) 82–87.
[16] M.G. Nair, M. Nirmala, K. Rekha, A. Anukaliani, Structural, optical, photo catalytic and antibacterial activity of ZnO and Co doped ZnO nanoparticles, Mater. Lett., 65 (2011) 1797–1800.
[17] N. Al-Hardan, M.J. Abdullah, A. Abdul Aziz, H. Ahmad, Low operating temperature of oxygen gas sensor based on undoped and Cr-doped ZnO films, Appl. Surf. Sci., 256 (2010) 3468–3471.
[18] I. Djerdj, G. Garnweitner, D. Arčon, M. Pregelj, Z. Jagličić, M. Niederberger, Diluted magnetic semiconductors: Mn/Co-doped ZnO nanorods as case study, J. Mater. Chem., 43 (2008) 5208–5217.
[19] Q. Wan, K. Yu, T.H. Wang, C.L. Lin, Low-field electron emission from tetrapod-like ZnO nanostructures synthesized by rapid evaporation, Appl. Phys. Lett., 83 (2003) 2253–2255.
[20] M.L. Zheng, L.D. Zhang, G.H. Li, W.Z. Shen, Fabrication and optical properties of large-scale uniform zinc oxide nanowire arrays by one-step electrochemical deposition technique, Chem. Phys. Lett., 363 (2002) 123–128.
[21] J.-H. Lee, K.-H. Ko, B.-O. Park, Electrical and optical properties of ZnO transparent conducting films by the sol–gel method, J. Cryst. Growth, 247 (2003) 119–125.
[22] J.-J. Wu, S.-C. Liu, Low-temperature growth of well-aligned ZnO nanorods by chemical vapor deposition, Adv. Mater., 14 (2002) 215–218.
[23] J. Zhang, D.L. Sun, J.L. Yin, H.L. Su, C.S. Liao, C.H. Yan, Control of ZnO morphology via a simple solution route, Chem. Mater., 14 (2002) 4172–4177.
[24] K.H. Tam, C.K. Cheung, Y.H. Leung. A.B. Djurisić, C.C. Ling, C.D. Beling, S. Fung, W.M. Kwok, W.K. Chan, D.L. Phillips, L. Ding, W.K. Ge, Defects in ZnO nanorods prepared by a hydrothermal method, J. Phys. Chem. B, 110 (2006) 20865–20871.
[25] B. Xiang, P. Wang, X. Zhang, S.A. Dayeh, D.P.R. Aplin, C. Soci, D. Yu, D. Wang, Rational synthesis of p-type zinc oxide nanowire arrays using simple chemical vapor deposition, Nano. Lett., 7 (2007) 323–328.
[26] K.D. Bhatte, D.N. Sawant, R.A. Watile, B.M. Bhanage, A rapid, one step microwave assisted synthesis of nanosize zinc oxide, Mater. Lett., 69 (2012) 66–68.
[27] F.K. Liu, P.W. Huang, Y.C. Chang, C.J. Ko, F.H. Ko, T.C. Chu, Formation of silver nanorods by microwave heating in the presence of gold seeds, J. Cryst. Growth, 273 (2005) 439–445.
[28] Y. Liu, J.H. Yang, Q.F. Guan, L.L. Yang, H.L. Liu, Y.J. Zhang, Y.X. Wang, D.D. Wang, J.H. Lang, Y.T. Yang, L.H. Fei, M.B. Wei, Effect of annealing temperature on structure, magnetic properties and optical characteristics in Zn0.97Cr0.03O nanoparticles, Appl. Surf. Sci., 256 (2010) 3559–3562.
[29] A. Meng, J. Xing, Z.J. Li, Q. Li, Cr-doped ZnO NPs: Synthesis, characterization, adsorption property and recycle, ACS Appl. Mater. Interfaces, 7 (2015) 27449–27457.
[30] Y.B. Li, Y. Li, M.Y. Zhu, T. Yang, J. Huang, H.M. Jin, Y.M. Hu, Structure and magnetic properties of Cr-doped ZnO nanoparticles prepared under high magnetic field, Solid State Commun., 150 (2010) 751–754.
[31] J. Zhu, Z. Deng, F. Chen, J. Zhang, H. Chen, M. Anpo, J. Huang, L. Zhang, Hydrothermal doping method for preparation of Cr^{3+}-TiO_2 photocatalysts with concentration gradient distribution of Cr^{3+}, Appl. Catal. B: Environ., 62 (2006) 329–335.
[32] W.J. Ong, S.Y. Voon, L.L. Tan, B.T. Goh, S.T. Yong, Enhanced daylight-induced photocatalytic activity of solvent exfoliated graphene (SEG)/ZnO hybrid nanocomposites toward degradation of reactive black 5, Ind. Eng. Chem. Res., 53 (2014) 17333–17344.

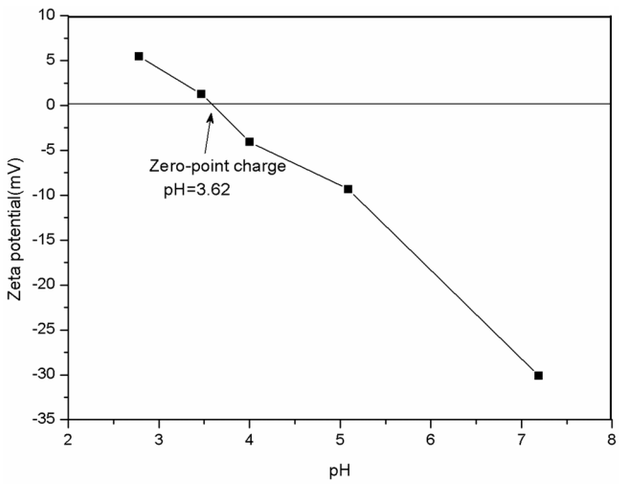

Fig. S1.

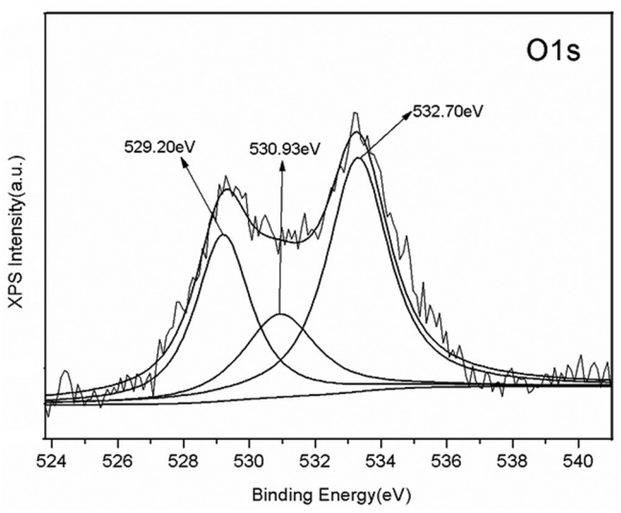

Fig. S2.

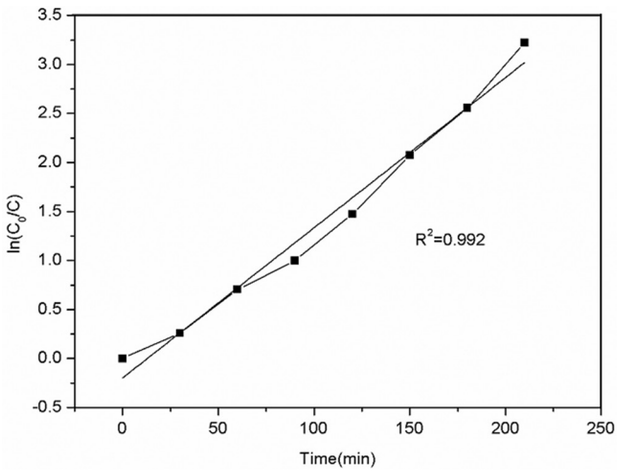

Fig. S3.

Table S1
Doped content of Cr^{3+} in ZnO (after three cycles)

Catalyst	2% Cr-ZnO
Theoretical content (mol%)	2.0
Actual content (mol%)	1.82